Eur. Phys. J. C (2023) 83:54
https://doi.org/10.1140/epjc/s10052-023-11223-5

THE EUROPEAN PHYSICAL JOURNAL C

Check for updates

Regular Article - Theoretical Physics

Precision studies for string derived Z' dynamics at the LHC

Andrew McEntaggart[1,2], **Alon E. Faraggi**[3], **Marco Guzzi**[1,a]

[1] Department of Physics, Kennesaw State University, Kennesaw, GA 30144, USA
[2] Department of Physics, Georgia Institute of Technology, Atlanta, GA 30332, USA
[3] Department of Mathematical Sciences, University of Liverpool, Liverpool L69 7ZL, UK

Received: 5 December 2022 / Accepted: 12 January 2023 / Published online: 21 January 2023
© The Author(s) 2023

Abstract We consider Z's in heterotic string derived models and study Z' resonant production at the TeV scale at the Large Hadron Collider (LHC). We use various kinematic differential distributions for the Drell–Yan process at NNLO in QCD to explore the parameter space of such models and investigate Z' couplings. In particular, we study the impact of Z-Z' kinetic-mixing interactions on forward-backward asymmetry (A_{FB}) and other distributions at the LHC.

1 Introduction

With the observation of a scalar particle compatible with the Standard Model electroweak Higgs doublet, the last piece in the Standard Model has been confirmed experimentally, and in the coming years its basic properties will be probed and elucidated. Furthermore, the discovery of the Higgs particle at 125 GeV suggests that the electroweak symmetry breaking mechanism is perturbative, rather than non-perturbative. This supports the old expectation that the Standard Model may provide viable parameterisation of particle physics data up to the Planck scale, where gravitational effects break the effective field theory description. Alas, the question remains how the Higgs mass and the ensuing electroweak symmetry breaking scales are protected from radiative corrections from the higher energy scale. While not yet seen at low energy experiments, supersymmetry remains one of the most appealing extensions of the Standard Model to address this puzzle. Furthermore, many supersymmetric models in fact predict that the Higgs particle should exist below 135 GeV. The observed Higgs particle is therefore compatible with supersymmetry. However, while supersymmetry protects the Higgs mass at the multi-loop level in the perturbative expansion, it introduces a problem at tree level, which is known as the μ-problem. Supersymmetry mandates the existence of a pair of Higgs doublets, which can receive a bilinear mass term in the superpotential. In the Minimal Supersymmetric Standard Model, the μ-parameter is therefore set by hand to be of the order of the electroweak scale, but nothing prevents it from being of the order of the Planck scale. Furthermore, absence of global symmetries in quantum gravity and the experience from quasi-realistic string derived models, do in fact suggest that generically the μ-parameter will be of that order. A possible solution to the problem may be obtained if the Higgs states are chiral under an additional $U(1)$ symmetry, which remains unbroken down to TeV scale. In this case, the bi-linear mass term for the supersymmetric Higgs pair can only be generated by the vacuum Expectation Value (VEV) that breaks the extra $U(1)$ symmetry.

String theory provides the most developed framework to study the incorporation of the Standard Model in a perturbatively consistent theory of quantum gravity. Indeed, over the past few decades detailed phenomenological models have been built that produce the spectrum of the Minimal Supersymmetric Standard Model (MSSM) in the effective low energy field theory limit below the Planck scale (for review and references see e.g. [1]). The heterotic-string models constructed in the free fermionic formulation [2–5], which are $Z_2 \times Z_2$ orbifolds of six dimensional toroidal spaces [6], are among the most realistic models constructed to date, and give rise to an abundance of three generation models with different unbroken $SO(10)$ subgroups below the string scale. However, the construction of string models with additional $U(1)$ gauge symmetries, that may stay unbroken down to low scales, has proven to be a difficult task [7,8]. The reason is that the extra $U(1)$ gauge symmetries that are often discussed in the context of Grand Unified Theory (GUT) extensions of the Standard Model are anomalous in explicit string models and therefore cannot remain unbroken down to low scales. In fact to date, there exist a single string derived model in which the extra $U(1)$ is anomaly free and can remain unbroken down

[a] e-mail: mguzzi@kennesaw.edu (corresponding author)

to the TeV scale [9]. As a bonus the string derived model predicts the existence of electroweak doublet pairs at the Z' breaking scale, that are chiral under the extra $U(1)$ symmetry. The bilinear mass term for these electroweak Higgs doublets can therefore be generated only by the VEV that breaks the extra $U(1)$ symmetry.

In this paper, we therefore study some of the properties of the extra $U(1)$ symmetry predicted by the string model and explore the parameter space of the Z' by using various kinematic distributions of resonant lepton-pair production in the Drell–Yan (DY) process at the LHC. Other related literature can be found in Refs. [10–13]. In addition, we study the effect of gauge kinetic-mixing interactions $\chi F^{\mu\nu} F'_{\mu\nu}$ in the lagrangian [14]. The impact of such a renormalizable operator is interesting in this context because it may in general be produced (at both field theory or string theory level) by physics at high scales above the Z' breaking scale, with no suppression by the large-mass scale [15,16] and can impact the couplings of Z's at the TeV scale [17]. The interplay between the gauge kinetic-mixing parameter and coupling of the Z', as well as other Z' properties, can be explored by using forward-backward asymmetry (A_{FB}) distributions in DY, where this observable can be advantageous in extra-resonance searches and as a model discrimination tool [18–28].

This paper is organized as follows. In Sect. 2 we describe the structure of the string derived Z' model. In Sect. 3 we discuss the phenomenological aspects of the model and analyze kinetic mixing. In Sect. 4 we illustrate and discuss our results. Finally, in Sect. 5 we present our conclusions.

2 The string model

We elaborate in this section on the structure of the string derived Z' model [9]. The model was constructed in the free fermionic formulation [29–31]. Only the important points relevant for the properties of the extra Z' gauge boson at low scales are discussed here and further details can be found in the original literature. Particularly relevant for the low energy phenomenology is the precise combination of worldsheet $U(1)$ currents predicted by the string model. In this respect we note that while similar aspects can be discussed in field theory models, in the string model the $U(1)$ combination is forced due to the available scalar multiplets to break the GUT symmetry, whereas in field theory models the scalar multiplets are a matter of choice.

In the free fermionic formulation all the worldsheet degrees of freedom required to cancel the conformal anomaly are represented in terms of free fermions propogating on the string worldsheet. In the standard notation the 64 worldsheet fermions in the lightcone gauge are denoted as:

Left-Movers: $\psi^{\mu}, \ \chi_i, \ y_i, \ \omega_i \quad (\mu = 1, 2, \ i = 1, \ldots, 6)$

Right-Movers

$$\bar{\phi}_{A=1,\ldots,44} = \begin{cases} \bar{y}_i \ , \ \bar{\omega}_i & i = 1, \ldots, 6 \\ \bar{\eta}_i & i = 1, 2, 3 \\ \bar{\psi}_{1,\ldots,5} & \\ \bar{\phi}_{1,\ldots,8} & \end{cases}$$

where the $\{y, \omega | \bar{y}, \bar{\omega}\}^{1,\ldots,6}$ correspond to the six dimensions of the internally compactified manifold; $\bar{\psi}^{1,\ldots,5}$ generate the $SO(10)$ GUT symmetry; $\bar{\phi}^{1,\ldots,8}$ generate the hidden sector gauge group; and $\bar{\eta}^{1,2,3}$ generate three $U(1)$ gauge symmetries. Models in the free fermionic formulation are defined in terms of boundary condition basis vectors, which specify the transformation properties of the worldsheet fermions around the noncontractible loops of the vacuum to vacuum amplitude, and the Generalised GSO projection coefficients of the one loop partition function [29–31]. The free fermion models are $Z_2 \times Z_2$ orbifold of six dimensional toroidal manifolds with discrete Wilson lines [6].

The Standard Model particle charges and data motivates the embedding of the Standard Model states in representations of Grand Unified Theories, like $SO(10)$ and E_6. The rank of these groups exceeds that of the Standard Model, and therefore they predict the existence of additional gauge symmetries, beyond the Standard Model. Compactifications of the heterotic-string to four dimensions do in fact give rise to E_6 GUT like models [32], which gives rise to string inspired Z' models. The additional $U(1)$ symmetries in these string inspired models have an E_6 embedding and produced numerous papers since the mid-eighties (for reviews and references see e.g. [10,11,20,33–35]). The construction of string derived models that allow for an unbroken extra $U(1)$ symmetry to remain unbroken down to low scales proves, however, to be very difficult. The symmetry breaking pattern $E_6 \to SO(10) \times U(1)_A$ in the string derived models entails that $U(1)_A$ is anomalous and cannot be part of an unbroken $U(1)_{Z'}$ at low energy scales [36]. String derived models with anomaly free $U(1)_{Z'} \notin E_6$ were analysed in [7,37–39], but agreement with the measured values of $\sin^2(\theta)_W(M_Z)$ and $\alpha_s(M_Z)$ favours Z' models with E_6 embedding [8]. We remark that the anomaly free $U(1)$ combination of $U(1)_{B-L}$ and $U(1)_{T_{3_R}} \in SO(10)$ may in principle stay unbroken down to low energy scales [40]. However, adequate suppression of the left-handed neutrino masses is facilitated if this $U(1)$ symmetry is broken at a high energy scale [41]. Constructing string models that enable an extra $U(1) \in E_6$ symmetry to stay unbroken down to low energy scales necessitates the construction of string models in which $U(1)_A$ is anomaly free. One method of achieving this outcome is to enhance $U(1)_A$ to a non-Abelian gauge symmetry á la Ref. [42]. An alternative is the string derived model of Ref. [9] that uses the

Spinor-Vector Duality (SVD) that was observed in $Z_2 \times Z_2$ orbifolds [43–45]. The SVD is under the exchange of the total number of $(16+\overline{16})$ representations of $SO(10)$ with the total number of 10 representations, and is readily understood if we consider the enhancement of $SO(10) \times U(1)_A$ to E_6. The chiral and anti-chiral multiplets of E_6 decompose under $SO(10) \times U(1)$ as $27 = 16 + 10 + 1$ and $\overline{27} = \overline{16} + 10 + 1$. In this case the $\#_1$ of $(16 + \overline{16})$ and $\#_2$ of 10 multiplets are equal. The E_6 symmetry point in the moduli space corresponds to a self-dual point under the exchange of the total number of $SO(10)$ spinorial plus anti-spinorial, with the total number of vectorial, multiplets. Breaking the E_6 gauge symmetry to $SO(10) \times U(1)_A$ results in the projection of some of the spinorial and vectorial multiplets, which results in $U(1)_A$ being anomalous. However, there may exist vacua with equal numbers of $(16 + \overline{16})$ spinorial, and 10 vectorial, multiplets, and traceless $U(1)_A$, without enhancement of the $SO(10) \times U(1)_A$ symmetry to E_6 [9]. In such models the chiral spectrum still forms complete E_6 representations, but the gauge symmetry is not enhanced to E_6. In this cases $U(1)_A$ is anomaly free and may remain unbroken down to low scales.

A fishing algorithm to extract models with specified physical properties was developed by using the free fermionic model building rules [5,46–52]. In Ref. [9], using the free fermionic fishing algorithm, such a spinor-vector self dual model was obtained with subsequent breaking at the string scale of the $SO(10)$ symmetry to the $SO(6) \times SO(4)$ subgroup, and preserves the spinor-vector self-duality. This model is a string derived model in which an extra $U(1)$ with E_6 embedding may remain unbroken down to low scales. The full massless spectrum of the string derived model is given in Ref. [9]. The observable and hidden gauge groups at the string scale are produced by untwisted sector states and are given by:

$$\begin{aligned} &\text{observable}: \quad SO(6) \times SO(4) \times U(1)_1 \times U(1)_2 \times U(1)_3 \\ &\quad \text{hidden}: \quad\quad SO(4)^2 \times SO(8) \end{aligned}$$

The massless string spectrum contains the fields required to break the GUT symmetry to the Standard Model.

The string model contains two anomalous $U(1)$ symmetries

$$\mathrm{Tr}U(1)_1 = 36 \quad \text{and} \quad \mathrm{Tr}U(1)_3 = -36. \tag{1}$$

The E_6 combination, given by,

$$U(1)_\zeta \;=\; U(1)_1 + U(1)_2 + U(1)_3\,, \tag{2}$$

is anomaly free and can be part of an unbroken $U(1)$ symmetry below the string scale. The $SO(6) \times SO(4)$ observable gauge symmetry is broken by the VEVs of the heavy Higgs fields $\mathcal{H}$ and $\overline{\mathcal{H}}$. The charges of these fields under the Standard Model gauge group factors is given by:

$$\begin{aligned} \overline{\mathcal{H}}(\bar{\mathbf{4}}, \mathbf{1}, \mathbf{2}) \to\; & u^c_H \left(\bar{\mathbf{3}}, \mathbf{1}, \frac{2}{3}\right) + d^c_H \left(\bar{\mathbf{3}}, \mathbf{1}, -\frac{1}{3}\right) \\ & + \overline{\mathcal{N}}\,(\mathbf{1}, \mathbf{1}, 0) + e^c_H\,(\mathbf{1}, \mathbf{1}, -1) \\ \mathcal{H}\,(\mathbf{4}, \mathbf{1}, \mathbf{2}) \to\; & u_H \left(\mathbf{3}, \mathbf{1}, -\frac{2}{3}\right) + d_H \left(\mathbf{3}, \mathbf{1}, \frac{1}{3}\right) \\ & + \mathcal{N}\,(\mathbf{1}, \mathbf{1}, 0) + e_H\,(\mathbf{1}, \mathbf{1}, 1) \end{aligned}$$

The VEVs along the $\mathcal{N}$ and $\overline{\mathcal{N}}$ directions preserves $N = 1$ spacetime supersymmetry along a flat direction and leave the $U(1)$ combination

$$U(1)_{Z'} \;=\; \frac{1}{5}(U(1)_C - U(1)_L) - U(1)_\zeta \notin SO(10), \tag{3}$$

unbroken below the string scale. This $U(1)$ combination is anomaly free provided that $U(1)_\zeta$ is anomaly free, as is the case in the string derived model [9].

We emphasise that this symmetry breaking pattern, and the $U(1)_{Z'}$ combination in Eq. (3) is enforced in the string derived model due the available scalar states in the string spectrum to break the non-Abelian $SO(6) \times SO(4)$ gauge symmetry, and due to a doublet-triplet missing partner mechanism [53] that gives heavy mass to coloured scalar states that arise in the untwisted sector of the string model [9]. Thus, the combination given in Eq. (3) is the extra $U(1)$ combination that can arise in the string derived model with E_6 embedding of the charges. Contrary to the situation in string inspired model, where any combination of $U(1)_C - U(1)_L$ and $U(1)_\zeta$ is possible, the $U(1)$ combination $U(1)_{Z'}$ is the uniquely predicted combination in the string derived model.

Anomaly cancellation of the $U(1)_{Z'}$ gauge symmetry down to low scales, requires the vector-like leptons $\{H^i_{\rm vl}, \bar{H}^i_{\rm vl}\}$, and quarks $\{D^i\,, \overline{D}^i\}$, that are obtained from the vectorial 10 multiplets of $SO(10)$, and the $SO(10)$ singlets S^i in the 27 representation of E_6. The supermultiplet[1] states below the $SO(6) \times SO(4)$ breaking scale are displayed schematically in Table 1. The three right-handed neutrino N^i_L states obtain heavy mass at the $SU(2)_R$ breaking scale, which produces the seesaw mechanism [54]. The spectrum below the $SU(2)_R$ breaking scale is assumed to be supersymmetric. We include in the spectrum an additional pair of vector-like electroweak Higgs doublets, that facilitate gauge coupling unification at the GUT scale. This is justified in the string inspired models due to the string doublet-triplet splitting mechanism [55,56]. We note from Table 1 that this extra Higgs pair is not chiral with respect to $U(1)_{Z'}$, contrary to the three pairs, $\{H^i_{\rm vl}, \bar{H}^i_{\rm vl}\}$, that are chiral with respect to $U(1)_{Z'}$. Therefore, mass terms for these three pairs can only be generated by the breaking of $U(1)_{Z'}$, whereas the bilinear mass term for the extra vector-like Higgs pair can, in principle, be generated at a high scale. The states

[1] Superfields are indicated with a hat symbol.

Table 1 Supermultiplet spectrum and $SU(3)_C \times SU(2)_L \times U(1)_Y \times U(1)_{Z'}$ quantum numbers, with $i = 1, 2, 3$ for the three light generations. The charges are displayed in the normalisation used in free fermionic heterotic-string models

Field	$SU(3)_C$	$\times SU(2)_L$	$U(1)_Y$	$U(1)_{Z'}$
$\hat{Q}^i_L$	3	2	$+\frac{1}{6}$	$-\frac{2}{5}$
$\hat{u}^i_L$	$\bar{3}$	1	$-\frac{2}{3}$	$-\frac{2}{5}$
$\hat{d}^i_L$	$\bar{3}$	1	$+\frac{1}{3}$	$-\frac{4}{5}$
$\hat{e}^i_L$	1	1	$+1$	$-\frac{2}{5}$
$\hat{L}^i_L$	1	2	$-\frac{1}{2}$	$-\frac{4}{5}$
$\hat{D}^i$	3	1	$-\frac{1}{3}$	$+\frac{4}{5}$
$\hat{\bar{D}}^i$	$\bar{3}$	1	$+\frac{1}{3}$	$+\frac{6}{5}$
$\hat{H}^i_{\rm vl}$	1	2	$-\frac{1}{2}$	$+\frac{6}{5}$
$\hat{\bar{H}}^i_{\rm vl}$	1	2	$+\frac{1}{2}$	$+\frac{4}{5}$
$\hat{S}^i$	1	1	0	-2
$\hat{H}_1$	1	2	$-\frac{1}{2}$	$-\frac{4}{5}$
$\hat{H}_2$	1	2	$+\frac{1}{2}$	$+\frac{4}{5}$
$\hat{\phi}$	1	1	0	-1
$\hat{\bar{\phi}}$	1	1	0	$+1$
$\hat{\zeta}^i$	1	1	0	0

ϕ and $\bar{\phi}$ are exotic Wilsonian states [9,57]. Additionally, the existence of light states ζ_i, that are neutral under the $SU(3)_C \times SU(2)_L \times U(1)_Y \times U(1)_{Z'}$ low scale gauge group, is allowed. The $U(1)_{Z'}$ gauge symmetry can be broken at low scale by the VEV of the $SO(10)$ singlet fields S_i and/or $\phi_{1,2}$.

3 Phenomenological aspects of the model

In this section we illustrate details of the phenomenological analysis for the model described in the previous section whose charge assignment is given in Table 1. The analysis is based on previous work of two of the authors, published in Refs. [39,58–60] which is used as a reference for the notation. Some definitions are also imported for consistency.

3.1 Neutral gauge bosons sector

We start by analyzing the neutral gauge bosons sector. The covariant derivative relative to the low-scale gauge group $SU(3)_C \times SU(2) \times U(1)_Y \times U(1)_{Z'}$ is defined as

$$\mathcal{D}_\mu = \partial_\mu + i g_s A^a_\mu T^a + i g_2 W^a_\mu \tau^a + i g_Y \frac{Y}{2} A^Y_\mu + i g_{Z'} \frac{z}{2} B_\mu \tag{4}$$

where g_2 is the $SU(2)$ coupling and W^a_μ and τ^a are the $SU(2)$ gauge fields and generators respectively; g_Y is the $U(1)_Y$ coupling, while A^Y_μ is the gauge field and Y is the hypercharge. $g_{Z'}$ is the $U(1)_{Z'}$ coupling and B_μ and z are the gauge field and charge of the $U(1)_{Z'}$ respectively. g_s is the strong coupling constant, and A^a and T^a are the $SU(3)_C$ gauge fields and generators respectively.

The lagrangian of the Higgs sector is given

$$\mathcal{L} = \frac{1}{2} \left|\mathcal{D}_\mu H_1\right|^2 + \frac{1}{2} \left|\mathcal{D}_\mu H_2\right|^2 + \frac{1}{2} \sum_i \left|\mathcal{D}_\mu S_i\right|^2 \tag{5}$$

where the scalar components of the supermultiplets which give the two Higgs doublets are represented by the H_1 and H_2 fields, that have hypercharge $Y_{H1} = -1$, $Y_{H2} = 1$ and $U(1)_{Z'}$ charges z_{H1} and z_{H2}. The singlets are the S_i fields, and as in [58] we consider only one S field for simplicity. The hypercharge of S is $Y_S = 0$ and its charge under $U(1)_{Z'}$ is z_s.

The Higgs fields are parametrized as

$$\begin{aligned} H_1 &= \begin{pmatrix} \mathrm{Re}H_1^0 + i\mathrm{Im}H_1^0 \\ \mathrm{Re}H_1^- + i\mathrm{Im}H_1^- \end{pmatrix}, \\ H_2 &= \begin{pmatrix} \mathrm{Re}H_2^+ + i\mathrm{Im}H_2^+ \\ \mathrm{Re}H_2^0 + i\mathrm{Im}H_2^0 \end{pmatrix}, \\ S &= \mathrm{Re}S + i\mathrm{Im}S, \end{aligned} \tag{6}$$

and the vacuum expectation values (VEVs) are defined as

$$\langle H_1 \rangle = \begin{pmatrix} v_1 \\ 0 \end{pmatrix}, \quad \langle H_2 \rangle = \begin{pmatrix} 0 \\ v_2 \end{pmatrix}, \quad \langle S \rangle = v_s. \tag{7}$$

Expanding the Higgs lagrangian and collecting quadratic terms, we obtain the mass matrix in the $(W^3_\mu, A^Y_\mu, B_\mu)$ basis as

$$M^2 = \frac{1}{4} \begin{pmatrix} g_2^2 v^2 & -g_2 g_Y v^2 & g_2 x_z \\ -g_2 g_Y v^2 & g_Y^2 v^2 & -g_Y x_z \\ g_2 x_z & -g_Y x_z & N_z \end{pmatrix} \tag{8}$$

where for convenience we have defined the following quantities

$$\begin{aligned} v^2 &= v_1^2 + v_2^2, \quad x_z = g_{Z'}(z_{H1} v_1^2 - z_{H2} v_2^2), \\ N_z &= g_{Z'}^2 (z_{H1}^2 v_1^2 + z_{H2}^2 v_2^2 + z_s^2 v_s^2). \end{aligned} \tag{9}$$

The zero eigenvalue of the mass matrix corresponds to the photon. The other two eigenvalues correspond to the square mass of the Z and Z' physical gauge bosons

$$\begin{aligned} M_Z^2 &= \frac{1}{8} \left(g^2 v^2 + N_z - \sqrt{(N_z - g^2 v^2)^2 + 4 g^2 x_z^2} \right), \\ M_{Z'}^2 &= \frac{1}{8} \left(g^2 v^2 + N_z + \sqrt{(N_z - g^2 v^2)^2 + 4 g^2 x_z^2} \right) \end{aligned} \tag{10}$$

where $g^2 = g_2^2 + g_Y^2$. From Eq. 10 we see that the presence of the Z' induces corrections on the mass of the SM Z boson. In Fig. 1 we show the impact of these corrections on the SM Z boson mass within the current uncertainties reported in the PDG [61] as a function of $g_{Z'}$ for different values of $M_{Z'}$. We

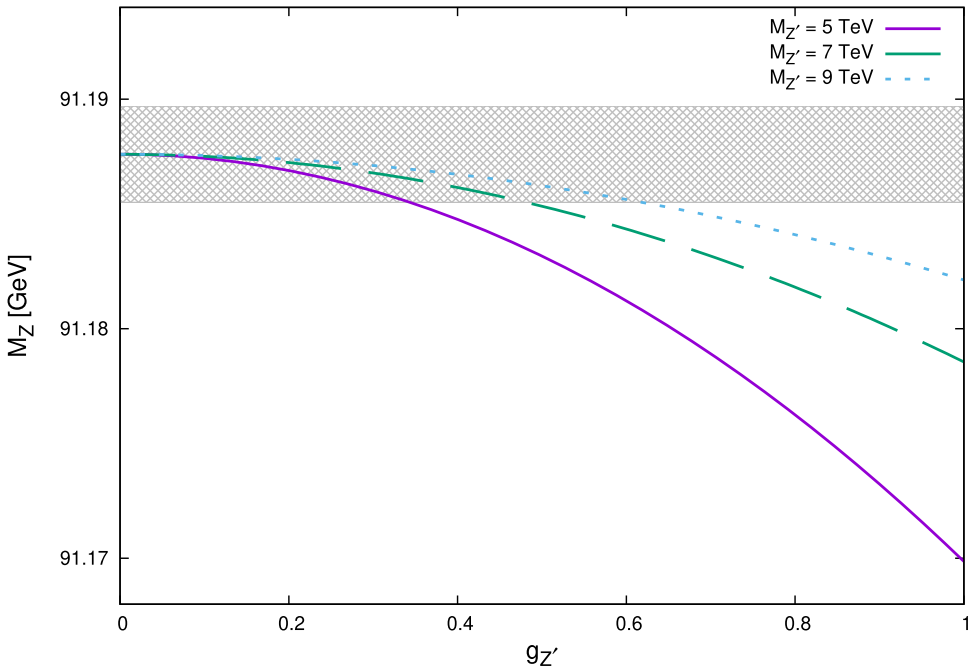

Fig. 1 Z'-induced corrections on the SM Z boson mass as a function of $g_{Z'}$ for fixed values of $M_{Z'}$. The hatched band represents the current measured M_Z uncertainty as reported in the PDG [61]

note that for $g_{Z'} \lesssim 0.4$ deviations are well within the current uncertainties.

In the limit where v_s is very large, the Z' mass decouples and one obtains simplified expressions for the gauge boson masses,

$$M_Z^2 = \frac{1}{4} g^2 v^2 \left[1 + \mathcal{O}(1/v_s^2)\right],$$
$$M_{Z'}^2 = \frac{1}{4} N_z \left[1 + \mathcal{O}(1/v_s^2)\right] \tag{11}$$

From the mass matrix diagonalization we obtain the normalized orthogonal eigenvector matrix which is used to rotate the gauge field basis to the physical field basis. The exact form of the elements of this matrix is given in Appendix A. When v_s is large, the rotation matrix can be simplified as

$$\begin{pmatrix} W_\mu^3 \\ A_\mu^Y \\ B_\mu \end{pmatrix} = \begin{pmatrix} \sin\theta_W & \cos\theta_W \cos\delta & \cos\theta_W \sin\delta \\ \cos\theta_W & -\sin\theta_W \cos\delta & -\sin\theta_W \sin\delta \\ 0 & -\sin\delta & \cos\delta \end{pmatrix} \times \begin{pmatrix} A_\mu^\gamma \\ Z_\mu \\ Z'_\mu \end{pmatrix} \tag{12}$$

where θ_W is the Weinberg angle, $\sin\theta_W = g_2/g$ and $\cos\theta_W = g_Y/g$ as in the Standard Model, and the small mixing between the Z and Z' is parametrized by the angle δ, defined by

$$\sin\delta = \frac{g x_z}{N_z - g^2 v^2} + \mathcal{O}\left(\frac{1}{v_s^2}\right) \tag{13}$$

To simplify the notation, we define a perturbative parameter $\varepsilon = \sin\delta$. The rotation matrix in Eq. 12 to first order in ε can now be written as

$$O_{gauge} = \begin{pmatrix} \sin\theta_W & \cos\theta_W & \varepsilon\cos\theta_W \\ \cos\theta_W & -\sin\theta_W & -\varepsilon\sin\theta_W \\ 0 & -\varepsilon & 1 \end{pmatrix} \tag{14}$$

According to the parameter space explored in this work, ε is typically $10^{-4} \lesssim \varepsilon \lesssim 10^{-3}$. After fields are rotated to the physical basis, the covariant derivative for the neutral current (NC) sector of Eq. 4 in terms of the mass eigenstate fields is given by

$$\begin{aligned} \mathcal{D}_\mu^{NC} = \partial_\mu &+ i\left(g_2 \sin\theta_W \tau^3 + g_Y \cos\theta_W \frac{Y}{2}\right) A_\mu^\gamma \\ &+ i\left(g_2 \cos\theta_W \tau^3 - g_Y \sin\theta_W \frac{Y}{2} - \varepsilon g_{Z'} \frac{z}{2}\right) Z_\mu \\ &+ i\left(\varepsilon g_2 \cos\theta_W \tau^3 - \varepsilon g_Y \sin\theta_W \frac{Y}{2} + g_{Z'} \frac{z}{2}\right) Z'_\mu \end{aligned} \tag{15}$$

The neutral current contributions in the Lagrangian, that are of the form $\bar\psi \gamma^\mu c^Z \psi Z_\mu$ and $\bar\psi \gamma^\mu c^{Z'} \psi Z'_\mu$, can be rewritten using the relations $g_Y \cos\theta_W = g_2 \sin\theta_W$, $Q = \tau^3 + \frac{Y}{2}$, $e = g_2 \sin\theta_W$

$$\begin{aligned} c^Z &= g(\tau^3 - \sin^2\theta_W Q) - \varepsilon g_{Z'} \frac{z}{2} \\ c^{Z'} &= \varepsilon g(\tau^3 - \sin^2\theta_W Q) + g_{Z'} \frac{z}{2} \end{aligned} \tag{16}$$

where the charges τ^3, Q, z correspond to the fermion and ε is the (small) mixing parameter. Using this notation, the interactions between fermions and electroweak neutral gauge bosons are expressed in terms of the vector and axial vector couplings, i.e., $\bar\psi \gamma^\mu \frac{g}{4} \left(g_V^Z - g_A^Z \gamma^5\right) \psi Z_\mu$ and

$\bar{\psi}\gamma^\mu \frac{g}{4}\left(g_V^{Z'} - g_A^{Z'}\gamma^5\right)\psi Z'_\mu$. These couplings are explicitly given as

$$\begin{aligned}
\frac{g}{4}g_V^Z &= \frac{1}{2}\left[g\left(\tau_L^3 - 2\sin^2\theta_W Q\right) - \varepsilon g_{Z'}\left(\frac{z_L}{2}+\frac{z_R}{2}\right)\right]\\
\frac{g}{4}g_A^Z &= \frac{1}{2}\left[g\tau_L^3 - \varepsilon g_{Z'}\left(\frac{z_L}{2}-\frac{z_R}{2}\right)\right]\\
\frac{g}{4}g_V^{Z'} &= \frac{1}{2}\left[\varepsilon g\left(\tau_L^3 - 2\sin^2\theta_W Q\right) + g_{Z'}\left(\frac{z_L}{2}+\frac{z_R}{2}\right)\right]\\
\frac{g}{4}g_A^{Z'} &= \frac{1}{2}\left[\varepsilon g\tau_L^3 + g_{Z'}\left(\frac{z_L}{2}-\frac{z_R}{2}\right)\right] \qquad (17)
\end{aligned}$$

where τ_L^3, $z_{L/R}$ refer to left/right-handed fermions.

3.2 Kinetic mixing

In this section we generalize the results obtained in the previous section to the case of kinetic-mixing interactions. The impact of kinetic mixing is assessed in Sect. 4, where applications to hadron collider phenomenology are discussed.

Since the low-energy gauge group includes two abelian groups, the Lagrangian for the kinetic terms can include a contribution which directly couples the A^Y and B fields and does not break either $U(1)_Y$ or $U(1)_{Z'}$ gauge invariance. This term corresponds to gauge kinetic mixing and is of the form

$$\Delta\mathcal{L}_{kin} = -\chi A^Y_{\mu\nu}B^{\mu\nu} \qquad (18)$$

where $A^Y_{\mu\nu}$ and $B_{\mu\nu}$ are the field-strength tensors for the $U(1)_Y$ and $U(1)_{Z'}$ symmetry groups respectively, and χ is a parameter such that $|\chi| < 1$. This renormalizable operator plays an interesting role in the context of our model because it can be produced at scales much higher than the Z' breaking scale and can affect the couplings of Z's at the TeV scale. It is therefore interesting to study the interplay between the gauge kinetic-mixing parameter and coupling of the Z'. The expression for the electroweak NC covariant derivative is generalized as

$$\mathcal{D}_\mu^{NC} = \partial_\mu + ig_2 W_\mu^3\tau^3 + iQ^T GA \qquad (19)$$

where $Q^T = (Y/2, z/2)$ is a vector containing the charges for the two $U(1)$ groups, G is the mixing matrix which is defined as

$$G = \begin{pmatrix} g_{AA} & g_{AB}\\ g_{BA} & g_{BB}\end{pmatrix} \qquad (20)$$

and contains the gauge couplings, and $A = (A_\mu^Y, B_\mu)^T$ contains the $U(1)$ gauge fields. The off-diagonal elements g_{AB} and g_{BA} contain the kinetic mixing between the $U(1)$ fields.

It is convenient to perform the rotation $A \to A' = RA$, $G \to G' = GR^{-1}$ where R is an orthogonal 2×2 matrix, and choose $g'_{BA} = 0$ in order to eliminate the $z_s g_{BA} A_\mu^Y$ term in $\mathcal{D}_\mu^{NC}$. This way, the Higgs singlet does not affect the $SU(2)\times U(1)_Y$ sector in the mass matrix. In the new basis, the mixing matrix reads

$$G' = \begin{pmatrix} g_Y & g_{KM}\\ 0 & g_{Z'}\end{pmatrix} \qquad (21)$$

where

$$\begin{aligned}
g_Y &= (g_{AA}g_{BB} - g_{AB}g_{BA})/\sqrt{g_{BB}^2 + g_{AB}^2}\\
g_{Z'} &= \sqrt{g_{BB}^2 + g_{BA}^2}\\
g_{KM} &= (g_{AA}g_{BA} + g_{AB}g_{BB})/\sqrt{g_{BB}^2 + g_{BA}^2} \qquad (22)
\end{aligned}$$

The electroweak NC covariant derivative becomes

$$\begin{aligned}
\mathcal{D}_\mu^{NC} &= \partial_\mu + ig_2 W_\mu^3\tau^3 + ig_Y\frac{Y}{2}A_\mu^{Y'}\\
&\quad + i\left(g_{Z'}\frac{z}{2} + g_{KM}\frac{Y}{2}\right)B'_\mu \qquad (23)
\end{aligned}$$

where $A_\mu^{Y'}$ and B'_μ are the rotated $U(1)$ gauge fields. Therefore, the inclusion of gauge kinetic mixing can be studied by using a single parameter g_{KM}. The mass matrix in the $(W_\mu^3, A_\mu^{Y'}, B'_\mu)$ basis is now

$$\frac{1}{4}\begin{pmatrix} g_2^2v^2 & -g_2g_Yv^2 & g_2x'_z\\ -g_2g_Yv^2 & g_Y^2v^2 & -g_Yx'_z\\ g_2x'_z & -g_Yx'_z & N'_z\end{pmatrix} \qquad (24)$$

where x_z and N_z have been replaced by their primed expressions given by

$$\begin{aligned}
x'_z &= g_{Z'}(z_{H1}v_1^2 - z_{H2}v_2^2) - g_{KM}v^2\\
N'_z &= (g_{Z'}z_{H1} - g_{KM})^2v_1^2 + (g_{Z'}z_{H2} + g_{KM})^2v_2^2\\
&\quad + g_{Z'}^2z_s^2v_s^2 \qquad (25)
\end{aligned}$$

The calculation for the gauge boson masses and the rotation matrix to the physical gauge boson basis proceeds identically to the previous section, with the replacements $x_z \to x'_z$ and $N_z \to N'_z$. With these modifications, the general form of the fermionic couplings to the Z and Z' in presence of kinetic mixing is

$$\begin{aligned}
c^Z &= g(\tau^3 - \sin^2\theta_W Q) - \varepsilon'\left(g_{Z'}\frac{z}{2} + g_{KM}\frac{Y}{2}\right)\\
c^{Z'} &= \varepsilon' g(\tau^3 - \sin^2\theta_W Q) + g_{Z'}\frac{z}{2} + g_{KM}\frac{Y}{2}, \qquad (26)
\end{aligned}$$

where the perturbative parameter from the previous section is modified as

$$\varepsilon' = \frac{gx'_z}{N'_z - g^2v^2} + \mathcal{O}\left(\frac{1}{v_s^2}\right) \qquad (27)$$

The vector and axial vector couplings of the gauge bosons to the fermions are now

$$\begin{aligned}
\frac{g}{4}g_V^Z &= \frac{1}{2}\Bigg[g\left(\tau_L^3 - 2\sin^2\theta_W Q\right)\\
&\quad - \varepsilon' g_{Z'}\left(\frac{z_L}{2}+\frac{z_R}{2}\right) - \varepsilon' g_{KM}\left(\frac{Y_L}{2}+\frac{Y_R}{2}\right)\Bigg]
\end{aligned}$$

$$\begin{aligned}
\frac{g}{4}g_A^Z &= \frac{1}{2}\left[g\tau_L^3 - \varepsilon' g_{Z'}\left(\frac{z_L}{2} - \frac{z_R}{2}\right)\right. \\
&\quad \left. -\varepsilon' g_{KM}\left(\frac{Y_L}{2} - \frac{Y_R}{2}\right)\right] \\
\frac{g}{4}g_V^{Z'} &= \frac{1}{2}\left[\varepsilon' g\left(\tau_L^3 - 2\sin^2\theta_W Q\right)\right. \\
&\quad \left. +g_{Z'}\left(\frac{z_L}{2} + \frac{z_R}{2}\right) + g_{KM}\left(\frac{Y_L}{2} + \frac{Y_R}{2}\right)\right] \\
\frac{g}{4}g_A^{Z'} &= \frac{1}{2}\left[\varepsilon' g\tau_L^3 + g_{Z'}\left(\frac{z_L}{2} - \frac{z_R}{2}\right)\right. \\
&\quad \left. +g_{KM}\left(\frac{Y_L}{2} - \frac{Y_R}{2}\right)\right] \qquad (28)
\end{aligned}$$

4 Hadron collider phenomenology applications

In this section we explore the parameter space of the model and perform a detailed analysis for proton-proton collisions at the LHC using Drell–Yan (DY) kinematic distributions calculated at the next-to-next-to-leading order (NNLO) in the strong coupling constant α_s of Quantum Chromodynamics (QCD). The contribution of electroweak corrections is not considered here and their impact will be analyzed in a forthcoming work. We explore the sensitivity of the forward-backward asymmetry (A_{FB}) distribution to the Z' and its parameters. In particular, we use A_{FB} distributions to study the interplay between the gauge kinetic-mixing parameter and coupling of the Z'. It has been pointed out in several works (e.g., see [18–28] and references therein) that A_{FB} distributions are very sensitive to SM deviations in the electroweak sector, and in particular to the presence of extra gauge vector bosons. Moreover, the ATLAS, LHCb, and CMS collaborations at the LHC have performed high-precision measurements of A_{FB} distributions at 7, 8, and 13 TeV collision energy respectively [62–64]. The CMS collaboration [64] has recently set lower limits on the mass of additional gauge bosons from sequential SM extensions at around 4.4 TeV.

Our theory predictions for the DY cross section are complemented by the calculation of uncertainties induced by parton distribution functions (PDFs) in the proton, as well as scale uncertainties for some of the distributions. PDFs represent one of the major sources of uncertainty in cross section calculations and complicate model validation and discrimination. The expression for the DY cross section in QCD factorization can be written as

$$\begin{aligned}
d\sigma &= \sum_{ij}\int_0^1 dx_1 dx_2 f_i^{H_1}(x_1,\mu_F^2) f_j^{H_2}(x_2,\mu_F^2) \\
&\quad \times d\hat{\sigma}_{ij\to l\bar{l}}(x_1,x_2;\alpha_s(\mu_R^2),\mu_R^2,\mu_F^2) + \mathcal{O}\left(\frac{\Lambda_{\rm QCD}^2}{Q^2}\right) \qquad (29)
\end{aligned}$$

where $f_i^{H_1}$ and $f_j^{H_2}$ are the proton PDFs, which depend on the longitudinal momentum fraction x_1 and x_2 of parton i and j respectively, and on the factorization scale μ_F. $d\hat{\sigma}$ is the hard scattering cross section, which is perturbatively calculable in QCD, μ_R is the renormalization scale, and $\left(\Lambda_{\rm QCD}^2/Q^2\right)$ represents power-suppressed contributions where $\Lambda_{\rm QCD}$ is the QCD scale.

The calculation of the differential distributions at NNLO in QCD which we present in this work has been performed by using an amended version of the `MCFM-v9.0` computer program [65–69], which has been modified to incorporate the string-derived model with charge assignments in Table 1, the Z' contribution, as well as the interference terms. We validated this implementation against other computer programs such as `DY-Turbo` [70] and `FEWZ` [71,72] and found agreement within 1%. Our results are presented at $\sqrt{S} = 13$ TeV of center-of-mass energy and we used the CT18NNLO [73] PDFs with conservative uncertainties evaluated at the 90% confidence level (CL). As a case study, we have chosen a string-derived Z' with $M_{Z'} = 5$ TeV. The impact of other recent PDF determinations [74–76] on A_{FB} distributions in the context of extra resonance searches is studied in Refs. [27,28]. Scale uncertainties are obtained by using the 7-point variation, that is, varying μ_R and μ_F up and down independently by a factor of 2, and then taking the envelope.

For the scope of this analysis, it is sufficient to include in the total decay rate of the Z' entering the cross section calculation, only the major decay channels which we report in the expression below

$$\Gamma_{Z'} = \sum_f \Gamma_{Z'\to f\bar{f}} + \Gamma_{Z'\to W^+W^-} + \Gamma_{Z'\to H^+H^-}, \qquad (30)$$

where f runs over the quarks and leptons, $W^\pm$ are the charged gauge vector bosons, and $H^\pm$ are the Higgs bosons of the charged sector. The expression for the $\Gamma_{Z'\to H^+H^-}$ channel in presence of gauge kinetic mixing is given in Appendix B. The calculation of the partial rates relative to the other channels proceeds similarly to that in Refs. [58,60]: in the expression for the Z' decay rate in the fermion channel, the vector and axial vector couplings are replaced by those in Eq. 28, while in the expression for the rate in the W^+ W^- channel ε is replaced by ε' from Eq. 27.

4.1 Kinematic distribution results

In Fig. 2 we show the string-derived Z' results for the dilepton invariant mass (m_{ll}) DY spectrum at the LHC 13 TeV in the electron channel, for a Z' of mass $M_{Z'} = 5$ TeV and different values of the coupling $g_{Z'}$ and kinetic-mixing parameter g_{KM}. These theory predictions are compared to the SM and the cross sections are calculated in the full phase space. The error bands represent the CT18NNLO induced PDF uncer-

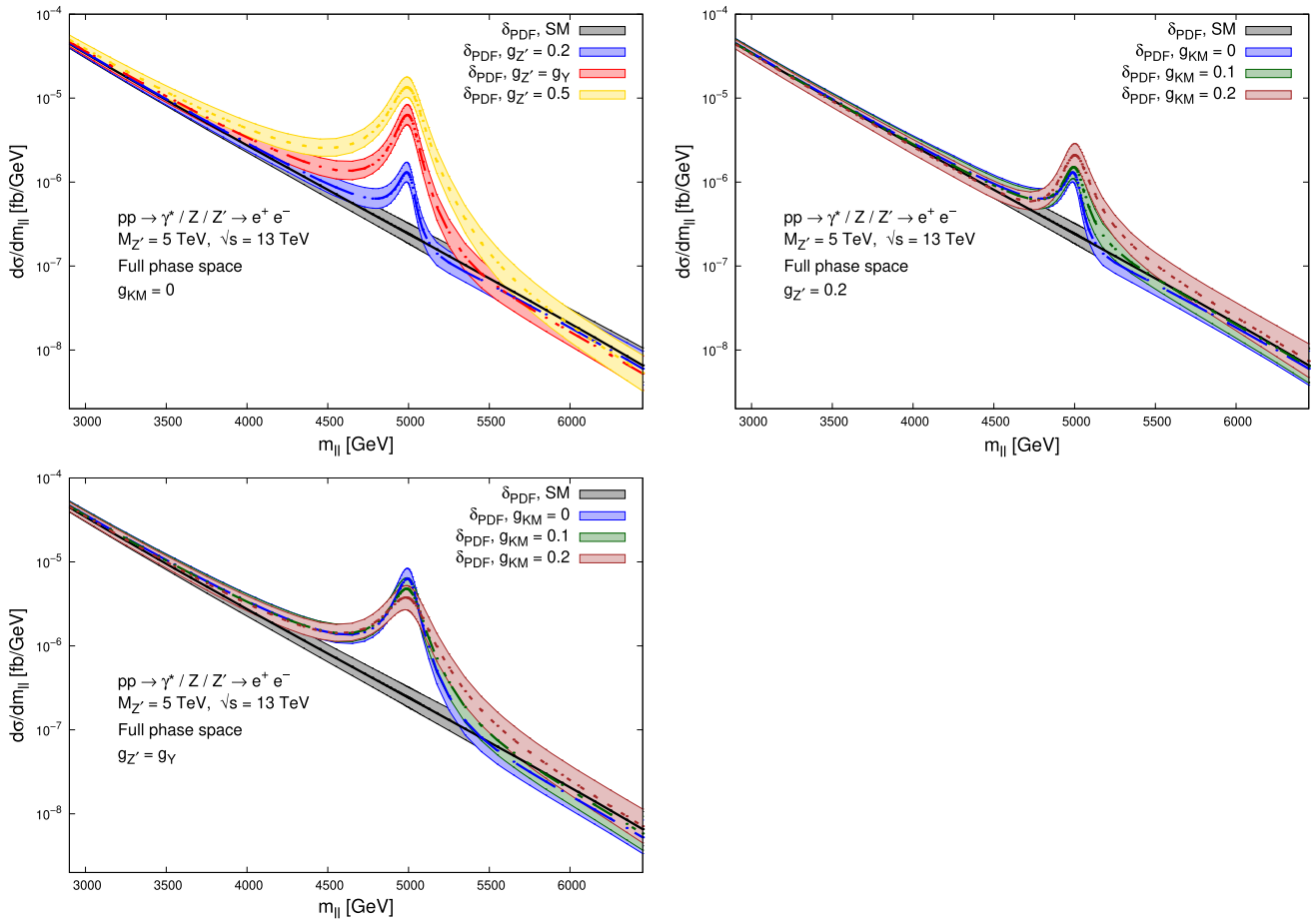

Fig. 2 Z' invariant mass distributions for varying $g_{Z'}$ and g_{KM}. The error bands represent the CT18NNLO induced PDF uncertainty on the cross section at 90% CL. Central predictions are represented by lines with different dashing

tainty evaluated at the 90% CL. Central predictions are represented by lines with different dashing. We observe how the interplay between g_{KM} and $g_{Z'}$ modifies the shape of the resonance and in particular the width for $g_{Z'} = 0.2$ and $g_{Z'} = g_Y$, when the strength of g_{KM} is varied. The inclusion of kinetic mixing has a significant effect on the width of the resonance in the invariant mass distribution.

It is interesting to explore the impact of varying these parameters on more differential observables such as the Z' transverse momentum p_T spectrum and the Z' rapidity distribution $y_{Z'}$, which we illustrate in Fig. 3. Here, the invariant mass of the final-state dilepton pair is chosen to be $4.6 < m_{l\bar{l}} < 5.4$ TeV. In the left-column insets, where $g_{KM} = 0$, PDF uncertainties are represented by red-hatched bands while scale uncertainties are represented by blue bands. In the right-column insets we illustrate for clarity the same distributions with no uncertainties but with $g_{KM} > 0$. We observe that kinetic mixing has negligible impact on these two distributions for this choice of the parameters in the kinematic region $4.6 < m_{l\bar{l}} < 5.4$ TeV. Again, we observe that PDF uncertainty dominates.

Finally, in Fig. 4 we show the impact of varying the $g_{Z'}$ and g_{KM} parameters on the $\cos\theta$ distribution, and on the pseudorapidity η_e spectrum of the final-state electron. The angle θ is defined in the Collins–Soper frame [77]. While there is almost no impact on the η_e spectrum, a distortion of the central value of the $\cos\theta$ angular distribution is observed when g_{KM} is progressively increased from 0 to 0.2. As we shall see in the next section, this is reflected by the A_{FB} distribution. However, all these effects in the $\cos\theta$ distribution are buried by the almost complete overlap of the PDF uncertainty bands for $g_{KM} = 0, 0.1, 0.2$.

4.2 Forward–backward asymmetry A_{FB} distribution results

As anticipated in the previous sections, a more suitable variable to explore the Z' parameters in DY is the forward-backward asymmetry A_{FB} distribution. This observable is a function of the chiral quark and lepton couplings to the mediating gauge bosons and is very sensitive to Z' properties. A_{FB} is expressed in terms of the difference between the

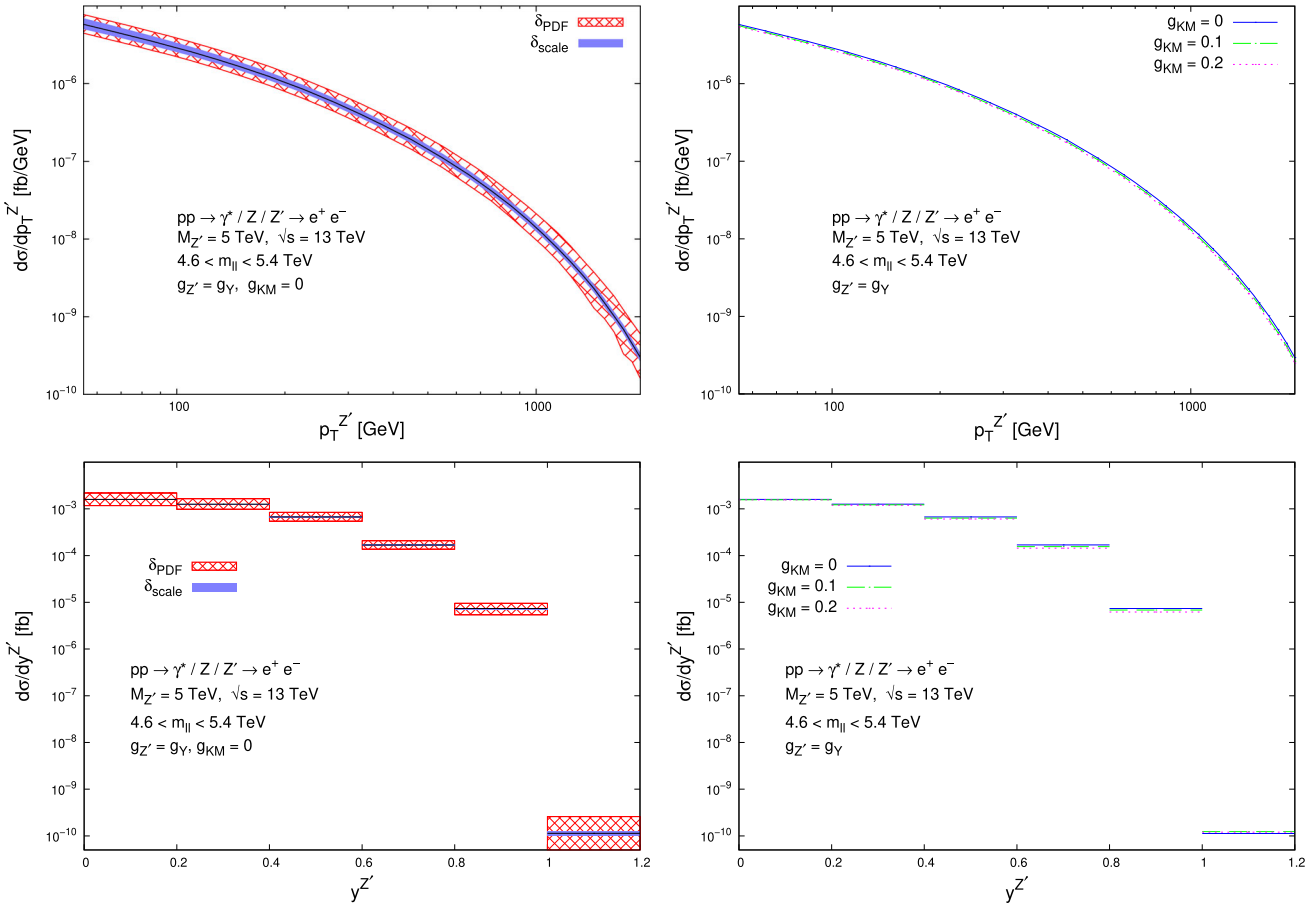

Fig. 3 Transverse momentum p_T (upper) and rapidity $y_{Z'}$ of the Z' (lower). The CT18NNLO PDF uncertainty is shown as a hatched red band and scale uncertainty is shown as a solid blue band. Central predictions are represented by a solid black line

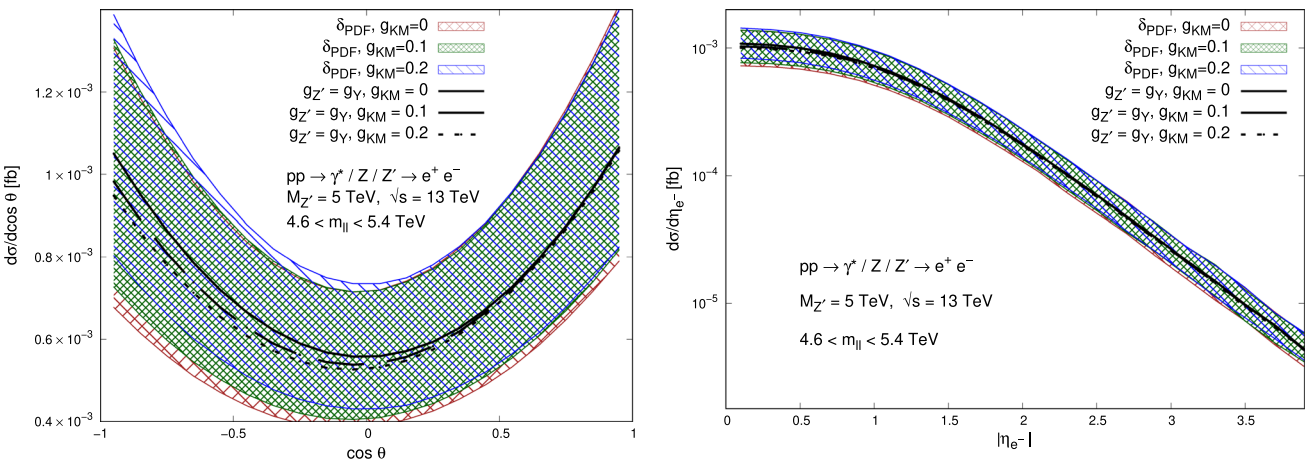

Fig. 4 Left: differential cross-section as a function of $\cos\theta$, where the θ angle is defined in the Collins–Soper frame. Right: pseudorapidity distribution η_e of the outgoing electron. Error bands with different hatching represent the CT18NNLO PDF uncertainties induced on the cross section, evaluated at the 90% CL. Central predictions are represented by lines with different dashing

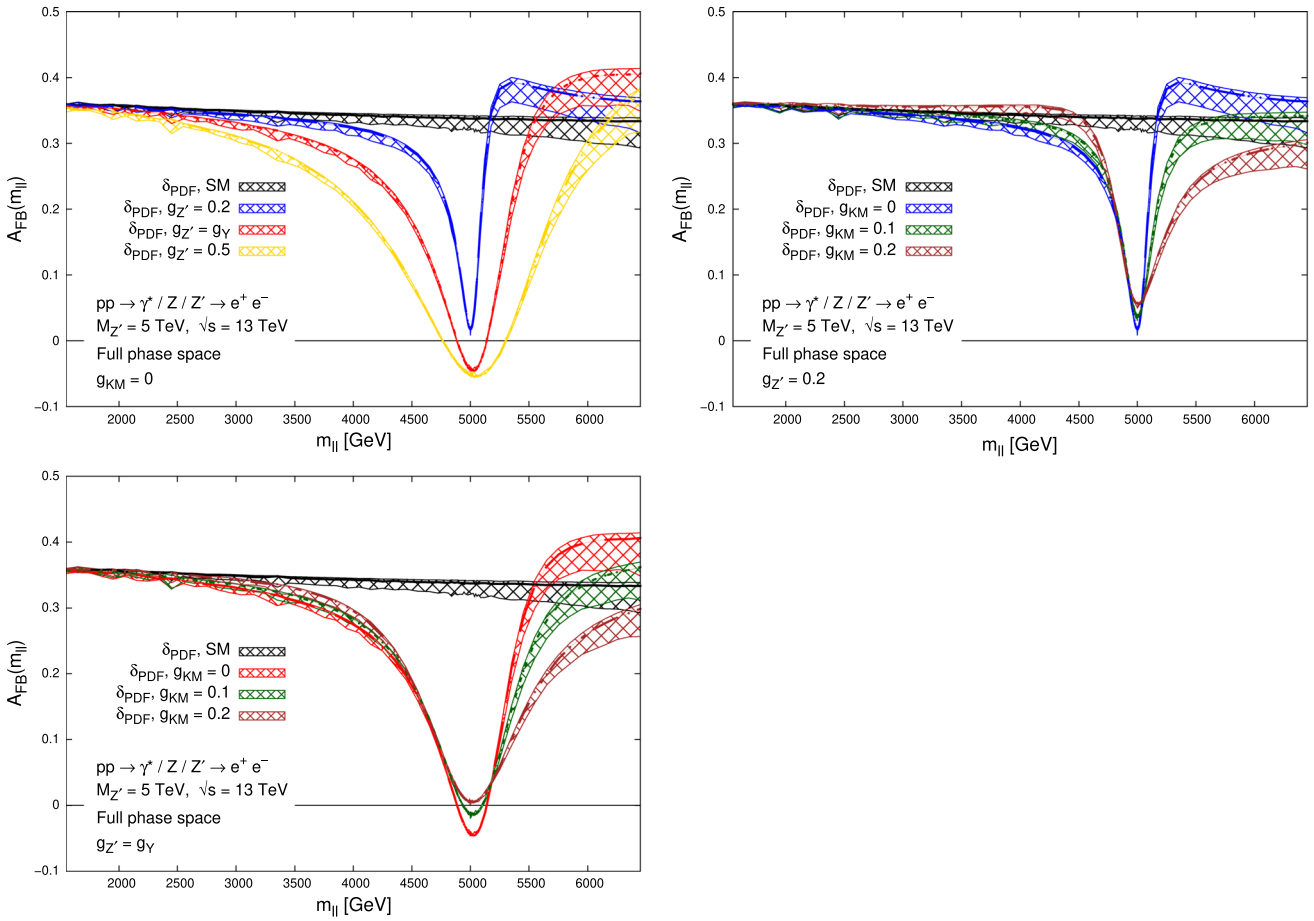

Fig. 5 Forward-backward asymmetry (A_{FB}) shown as a function of the dilepton invariant mass (m_{ll}) for different values of $g_{Z'}$ and g_{KM}. The black hatched band represents the Standard Model prediction. The solid black line at $A_{FB} = 0$ is introduced for reference. The CT18NNLO PDF uncertainties at the 90% CL are represented by hatched bands. Central predictions are shown as lines with different dashing

forward and backward angular contributions to the cross section, normalized to the total cross section. The forward and backward directions are represented by the angle θ between the negatively charged final-state lepton and the initial-state quark in the dilepton center-of-mass frame. A_{FB} is defined as

$$A_{FB} = \frac{d\sigma_F - d\sigma_B}{d\sigma_F + d\sigma_B} \tag{31}$$

where the forward ($d\sigma_F$) and backward ($d\sigma_B$) contributions are constructed by integrating the differential cross section over the forward and backward halves of the angular phase space

$$d\sigma_F = \int_0^1 \frac{d\sigma}{d\cos\theta_l} d\cos\theta_l,$$
$$d\sigma_B = \int_{-1}^0 \frac{d\sigma}{d\cos\theta_l} d\cos\theta_l. \tag{32}$$

θ_l is the angle between the final-state lepton and initial-state quark in the Collins–Soper frame. In our analysis, we study the A_{FB} distribution as a function of m_{ll}. In Fig. 5 we show the A_{FB} over the same invariant mass range adopted before. The presence of a Z' would lead to a distortion in the A_{FB} which becomes wider as $g_{Z'}$ increases. We calculated both

PDF and scale uncertainties for the A_{FB} distribution. Scale uncertainties are essentially invisible in Fig. 5, while PDF uncertainties are attenuated around the peak as compared to the distributions studied in the previous section, but are still large at high m_{ll}. Fig. 5 shows the sensitivity of A_{FB} to simultaneous variations of the $g_{Z'}$ and g_{KM} parameters. The distortions induced on the asymmetry tend to become shallower and wider as the kinetic mixing increases. Moving away from the resonance, when $g_{KM} \neq 0$, the discriminatory power of A_{FB} appears to be attenuated by PDF uncertainties.

5 Conclusions

In this work, we studied properties of heterotic string derived Z's in the TeV scale and explored their dynamics at the LHC. As a case study, we selected a Z' of mass $M_{Z'} = 5$ TeV. We analyzed the impact of a gauge kinetic-mixing term in the Lagrangian and its interplay with the Z' coupling. We explored the Z' parameter space the model in presence of kinetic mixing and performed a thorough phenomenological analysis in which we used precision calculations at NNLO in QCD to predict kinematic distributions for the Z' in the Drell–Yan process at the LHC. In particular, we exploited the sensitivity of forward-backward asymmetry A_{FB} distributions in Drell–Yan to further explore the parameter space and the interplay between the Z' coupling and the kinetic-mixing parameter. Moreover, we estimated theory uncertainties on the distributions from perturbative (scale dependence) and nonperturbative (PDFs in the proton) sources in QCD. Proton PDFs still remain one of the major sources of uncertainty in Z' searches. This is ascribed to the fact that the kinematic domain of heavy gauge boson production is sensitive, and is impacted by, PDFs at large x where uncertainties are still large due to lack of robust constraints from experimental data [78,79]. The motivation to consider the particular $U(1)_{Z'}$ combination in Eq. 3 stems from its extraction from a string derived heterotic-string model [9], in which it is the unique combination that may remain unbroken down to low scales. Its preservation as an unbroken gauge symmetry down to the TeV scale emanates from the role that it can play in suppressing some dangerous operators, like proton decay mediating operators, and furthermore by the role it can play in generating the electroweak symmetry breaking itself. Further analysis in that direction mandates the development of the interpolation tools between the string and electroweak scales and the extraction of further data from the string models. We note that while in this paper we treated the kinetic-mixing term as a free parameter, its computation, as that of many of the related parameters, can be obtained directly from the string models [16], hence increasing their predictive power. In this paper, we studied the case of Z' vector bosons that have an E_6 embedding. The advantage of this choice is that it facilitates gauge unification at the unification scale [8]. Such extra string inspired Z' models have been discussed extensively in the literature since the mid-eighties [20,33–35], but the combination given in Eq. 3 is obtained in the string derived model of Ref. [9]. Naturally, the string constructions can give rise to $U(1)$ symmetries with different characteristics and these have been of some interest in the literature [7,37–39]. The range of possibilities is more model dependent. The extra Z's in these cases can arise from flavour dependent $U(1)$ symmetries, as well as $U(1)$ symmetries that arise from the hidden sector of the heterotic-string. Naturally, the limits that we discussed in this paper will not apply to those cases (see for instance the discussion relative to Z' boson searches in the PDG [61] and references therein), as they do not couple universally to all the three families. On the other hand, there may exist other constraints in these cases arising from flavour non-universality and the need to break flavour dependent symmetries to produce viable fermion masses. Nevertheless, these cases do represent interesting alternatives to the family universal $U(1)$ and we will return to them in future work.

Acknowledgements The work of MG and AM is supported by the National Science foundation under Grant no. 2112025. The work of AF is supported in part by a Weston visiting professorship at the Weizmann Institute of Science. AF would like to thank Doron Gepner for discussions and the Department of Particle Physics and Astrophysics for hospitality.

Data Availability Statement This manuscript has no associated data or the data will not be deposited. [Authors' comment: This manuscript describes theory calculations in QCD and Beyond the Standard Model Physics and it does not require any data to be deposited.]

Open Access This article is licensed under a Creative Commons Attribution 4.0 International License, which permits use, sharing, adaptation, distribution and reproduction in any medium or format, as long as you give appropriate credit to the original author(s) and the source, provide a link to the Creative Commons licence, and indicate if changes were made. The images or other third party material in this article are included in the article's Creative Commons licence, unless indicated otherwise in a credit line to the material. If material is not included in the article's Creative Commons licence and your intended use is not permitted by statutory regulation or exceeds the permitted use, you will need to obtain permission directly from the copyright holder. To view a copy of this licence, visit http://creativecommons.org/licenses/by/4.0/.
Funded by SCOAP^3. SCOAP^3 supports the goals of the International Year of Basic Sciences for Sustainable Development.

Appendix A: Gauge boson rotation matrix components

In this section we report the exact components of the matrix $\mathcal{O}_{gauge}$ which rotates the neutral gauge field basis to the physical basis as in Eq. 12.

$$
\begin{aligned}
&\mathcal{O}_{11} = g_Y/g, \quad \mathcal{O}_{21} = g_2/g, \quad \mathcal{O}_{31} = 0,\\
&\mathcal{O}_{12} = -g_2 \frac{v^2\left(f_1+\sqrt{f_1^2+4g^2x_z^2}\right)-2x_z^2}{\sqrt{g^2\left[v^2\left(f_1+\sqrt{f_1^2+4g^2x_z^2}\right)-2x_z^2\right]^2+x_z^2\left(f_2-\sqrt{f_1^2+4g^2x_z^2}\right)^2}},\\
&\mathcal{O}_{22} = g_Y \frac{v^2\left(f_1+\sqrt{f_1^2+4g^2x_z^2}\right)-2x_z^2}{\sqrt{g^2\left[v^2\left(f_1+\sqrt{f_1^2+4g^2x_z^2}\right)-2x_z^2\right]^2+x_z^2\left(f_2-\sqrt{f_1^2+4g^2x_z^2}\right)^2}},\\
&\mathcal{O}_{32} = \frac{x_z\left(f_2-\sqrt{f_1^2+4g^2x_z^2}\right)}{\sqrt{g^2\left[v^2\left(f_1+\sqrt{f_1^2+4g^2x_z^2}\right)-2x_z^2\right]^2+x_z^2\left(f_2-\sqrt{f_1^2+4g^2x_z^2}\right)^2}},\\
&\mathcal{O}_{13} = -g_2 \frac{v^2\left(f_1-\sqrt{f_1^2+4g^2x_z^2}\right)-2x_z^2}{\sqrt{g^2\left[v^2\left(f_1-\sqrt{f_1^2+4g^2x_z^2}\right)-2x_z^2\right]^2+x_z^2\left(f_2+\sqrt{f_1^2+4g^2x_z^2}\right)^2}},\\
&\mathcal{O}_{23} = g_Y \frac{v^2\left(f_1-\sqrt{f_1^2+4g^2x_z^2}\right)-2x_z^2}{\sqrt{g^2\left[v^2\left(f_1-\sqrt{f_1^2+4g^2x_z^2}\right)-2x_z^2\right]^2+x_z^2\left(f_2+\sqrt{f_1^2+4g^2x_z^2}\right)^2}},\\
&\mathcal{O}_{33} = \frac{x_z\left(f_2+\sqrt{f_1^2+4g^2x_z^2}\right)}{\sqrt{g^2\left[v^2\left(f_1-\sqrt{f_1^2+4g^2x_z^2}\right)-2x_z^2\right]^2+x_z^2\left(f_2+\sqrt{f_1^2+4g^2x_z^2}\right)^2}}
\end{aligned}
\tag{A1}
$$

where $f_1 = N_z - g^2v^2$ and $f_2 = N_z + g^2v^2$. To include the effects of kinetic mixing on $\mathcal{O}_{gauge}$, we make the substitutions $x_z \to x_z'$ and $N_z \to N_z'$ as defined in Eq. 25.

Appendix B: $Z' \to H^+H^-$ decay rate

The decay rate of the Z' into charged Higgs bosons $Z' \to H^+H^-$ in presence of kinetic mixing is given by

$$
\Gamma_{Z'\to H^+H^-} = \frac{g^2_{Z'H^+H^-}}{16\pi^2 M^5_{Z'}}\left[M^2_{Z'}(M_{Z'}-2M_{H^\pm})(2M_{H^\pm}+M_{Z'})\right]^{3/2}, \tag{33}
$$

where the structure of the coupling is

$$
\begin{aligned}
g_{Z'H^+H^-} = &\left(\frac{v_1}{v}\right)^2(g_{Z'z_{H_1}}+\varepsilon g_2\cos\theta_W)\\
&+\left(\frac{v_2}{v}\right)^2(-g_{Z'z_{H_2}}+\varepsilon g_2\cos\theta_W)\\
&+(g_{KM}+\varepsilon g_Y\sin\theta_W)\left(\left(\frac{v_1}{v}\right)^2 Y_{H_1}\right.\\
&\left.-\left(\frac{v_2}{v}\right)^2 Y_{H_2}\right).
\end{aligned}
\tag{34}
$$

References

1. L.E. Ibanez, A.M. Uranga, *String Theory and Particle Physics: An Introduction to String Phenomenology* (Cambridge University Press, Cambridge, 2012), p.2
2. A.E. Faraggi, D.V. Nanopoulos, K.-J. Yuan, A Standard Like model in the 4D free fermionic string formulation. Nucl. Phys. B **335**, 347 (1990). https://doi.org/10.1016/0550-3213(90)90498-3

3. G.B. Cleaver, A.E. Faraggi, D.V. Nanopoulos, String derived MSSM and M theory unification. Phys. Lett. B **455**, 135 (1999). https://doi.org/10.1016/S0370-2693(99)00413-X. arXiv:hep-ph/9811427
4. A.E. Faraggi, Construction of realistic standard-like models in the free fermionic superstring formulation. Nucl. Phys. B **387**, 239 (1992). https://doi.org/10.1016/0550-3213(92)90160-D. arXiv:hep-th/9208024
5. A.E. Faraggi, J. Rizos, H. Sonmez, Classification of standard-like heterotic-string vacua. Nucl. Phys. B **927**, 1 (2018). https://doi.org/10.1016/j.nuclphysb.2017.12.006. arXiv:1709.08229
6. P. Athanasopoulos, A.E. Faraggi, S. GrootNibbelink, V.M. Mehta, Heterotic free fermionic and symmetric toroidal orbifold models. JHEP **04**, 038 (2016). https://doi.org/10.1007/JHEP04(2016)038. arXiv:1602.03082
7. A.E. Faraggi, V.M. Mehta, Proton stability and light Z' inspired by string derived models. Phys. Rev. D **84**, 086006 (2011). https://doi.org/10.1103/PhysRevD.84.086006. arXiv:1106.3082
8. A.E. Faraggi, V.M. Mehta, Proton stability, gauge coupling unification, and a light Z' in heterotic-string models. Phys. Rev. D **88**, 025006 (2013). https://doi.org/10.1103/PhysRevD.88.025006. arXiv:1304.4230
9. A.E. Faraggi, J. Rizos, A light Z' heterotic-string derived model. Nucl. Phys. B **895**, 233 (2015). https://doi.org/10.1016/j.nuclphysb.2015.03.031. arXiv:1412.6432
10. Y.Y. Komachenko, M.Y. Khlopov, On manifestation of Z' boson of heterotic string in exclusive neutrino $N \rightarrow$ neutrino P0 N processes. Sov. J. Nucl. Phys. **51**, 692 (1990)
11. Y.Y. Komachenko, M.Y. Khlopov, On manifestation of Z' boson of heterotic string in exclusive neutrino $N \rightarrow$ neutrino P0 N processes. Yad. Fiz. **51**, 1081 (1990)
12. A. Das, P.S.B. Dev, Y. Hosotani, S. Mandal, Probing the minimal $U(1)_X$ model at future electron-positron colliders via fermion pair-production channels. Phys. Rev. D **105**, 115030 (2022). https://doi.org/10.1103/PhysRevD.105.115030. arXiv:2104.10902
13. P. Anastasopoulos, F. Fucito, A. Lionetto, G. Pradisi, A. Racioppi, Y. Stanev, Minimal anomalous $U(1)'$ extension of the MSSM. Phys. Rev. D **78**, 085014 (2008). https://doi.org/10.1103/PhysRevD.78.085014. arXiv:0804.1156
14. B. Holdom, Two U(1)'s and epsilon charge shifts. Phys. Lett. B **166**, 196 (1986). https://doi.org/10.1016/0370-2693(86)91377-8
15. J. Polchinski, L. Susskind, Breaking of supersymmetry at intermediate-energy. Phys. Rev. D **26**, 3661 (1982). https://doi.org/10.1103/PhysRevD.26.3661
16. K.R. Dienes, C.F. Kolda, J. March-Russell, Kinetic mixing and the supersymmetric gauge hierarchy. Nucl. Phys. B **492**, 104 (1997). https://doi.org/10.1016/S0550-3213(97)00173-9. arXiv:hep-ph/9610479
17. T.G. Rizzo, Gauge kinetic mixing and leptophobic Z' in E(6) and SO(10). Phys. Rev. D **59**, 015020 (1998). https://doi.org/10.1103/PhysRevD.59.015020. arXiv:hep-ph/9806397
18. D. London, J.L. Rosner, Extra gauge bosons in E(6). Phys. Rev. D **34**, 1530 (1986). https://doi.org/10.1103/PhysRevD.34.1530
19. J.L. Rosner, Off peak lepton asymmetries from new Zs. Phys. Rev. D **35**, 2244 (1987). https://doi.org/10.1103/PhysRevD.35.2244
20. J.L. Hewett, T.G. Rizzo, Low-energy phenomenology of superstring inspired E(6) models. Phys. Rep. **183**, 193 (1989). https://doi.org/10.1016/0370-1573(89)90071-9
21. M. Cvetic, S. Godfrey, Discovery and identification of extra gauge bosons. Adv. Ser. Dir. High Energy Phys. **16**, 383 (1997). https://doi.org/10.1142/9789812830265_0007. arXiv:hep-ph/9504216
22. J.L. Rosner, Forward–backward asymmetries in hadronically produced lepton pairs. Phys. Rev. D **54**, 1078 (1996). https://doi.org/10.1103/PhysRevD.54.1078. arXiv:hep-ph/9512299
23. M. Dittmar, Neutral current interference in the TeV region: the experimental sensitivity at the LHC. Phys. Rev. D **55**, 161 (1997). https://doi.org/10.1103/PhysRevD.55.161. arXiv:hep-ex/9606002
24. A. Bodek, U. Baur, Implications of a 300-GeV/c to 500-Gev/c Z' boson on p antip collider data at $\sqrt{s} = 1.8$ TeV. Eur. Phys. J. C **21**, 607 (2001). https://doi.org/10.1007/s100520100778. arXiv:hep-ph/0102160
25. CDF collaboration, F. Abe et al., Search for new gauge bosons decaying into dileptons in $\bar{p}p$ collisions at $\sqrt{s} = 1.8$ TeV. Phys. Rev. Lett. **79**, 2192 (1997). https://doi.org/10.1103/PhysRevLett.79.2192
26. E. Accomando, A. Belyaev, J. Fiaschi, K. Mimasu, S. Moretti, C. Shepherd-Themistocleous, Forward–backward asymmetry as a discovery tool for Z' bosons at the LHC. JHEP **01**, 127 (2016). https://doi.org/10.1007/JHEP01(2016)127. arXiv:1503.02672
27. J. Fiaschi, F. Giuli, F. Hautmann, S. Moch, S. Moretti, $\mathbf{Z}'$-boson dilepton searches and the high-**x** quark density. arXiv:2211.06188
28. R.D. Ball, A. Candido, S. Forte, F. Hekhorn, E.R. Nocera, J. Rojo et al., Parton distributions and new physics searches: the Drell–Yan forward–backward asymmetry as a case study. arXiv:2209.08115
29. I. Antoniadis, C.P. Bachas, C. Kounnas, Four-dimensional superstrings. Nucl. Phys. B **289**, 87 (1987). https://doi.org/10.1016/0550-3213(87)90372-5
30. H. Kawai, D.C. Lewellen, S.H.H. Tye, Construction of fermionic string models in four-dimensions. Nucl. Phys. B **288**, 1 (1987). https://doi.org/10.1016/0550-3213(87)90208-2
31. I. Antoniadis, C. Bachas, 4-D fermionic superstrings with arbitrary twists. Nucl. Phys. B **298**, 586 (1988). https://doi.org/10.1016/0550-3213(88)90355-0
32. P. Candelas, G.T. Horowitz, A. Strominger, E. Witten, Vacuum configurations for superstrings. Nucl. Phys. B **258**, 46 (1985). https://doi.org/10.1016/0550-3213(85)90602-9
33. F. Zwirner, Phenomenological aspects of E_6 superstring-inspired models. Int. J. Mod. Phys. A **3**, 49 (1988). https://doi.org/10.1142/S0217751X88000035
34. A. Leike, The phenomenology of extra neutral gauge bosons. Phys. Rep. **317**, 143 (1999). https://doi.org/10.1016/S0370-1573(98)00133-1. arXiv:hep-ph/9805494
35. S.F. King, S. Moretti, R. Nevzorov, A review of the exceptional supersymmetric standard model. Symmetry **12**, 557 (2020). https://doi.org/10.3390/sym12040557. arXiv:2002.02788
36. G.B. Cleaver, A.E. Faraggi, On the anomalous U(1) in free fermionic superstring models. Int. J. Mod. Phys. A **14**, 2335 (1999). https://doi.org/10.1142/S0217751X99001172. arXiv:hep-ph/9711339
37. J.C. Pati, The essential role of string derived symmetries in ensuring proton stability and light neutrino masses. Phys. Lett. B **388**, 532 (1996). https://doi.org/10.1016/S0370-2693(96)01180-X. arXiv:hep-ph/9607446
38. A.E. Faraggi, Proton stability and superstring Z-prime. Phys. Lett. B **499**, 147 (2001). https://doi.org/10.1016/S0370-2693(01)00021-1. arXiv:hep-ph/0011006
39. C. Corianò, A.E. Faraggi, M. Guzzi, A novel string derived Z-prime with stable proton, light-neutrinos and R-parity violation. Eur. Phys. J. C **53**, 421 (2008). https://doi.org/10.1140/epjc/s10052-007-0469-2. arXiv:0704.1256
40. A.E. Faraggi, D.V. Nanopoulos, A SUPERSTRING Z' AT O (1-TeV)?? Mod. Phys. Lett. A **6**, 61 (1991). https://doi.org/10.1142/S0217732391002621
41. A.E. Faraggi, ν_τ mass as possible evidence for a superstring inspired standard like model. Phys. Lett. B **245**, 435 (1990). https://doi.org/10.1016/0370-2693(90)90670-2
42. L. Bernard, A.E. Faraggi, I. Glasser, J. Rizos, H. Sonmez, String derived exophobic $SU(6) \times SU(2)$ GUTs. Nucl. Phys. B **868**, 1 (2013). https://doi.org/10.1016/j.nuclphysb.2012.11.001. arXiv:1208.2145

43. A.E. Faraggi, C. Kounnas, J. Rizos, Spinor-vector duality in fermionic $Z(2) \times Z(2)$ heterotic orbifold models. Nucl. Phys. B **774**, 208 (2007). https://doi.org/10.1016/j.nuclphysb.2007.03.029. arXiv:hep-th/0611251
44. C. Angelantonj, A.E. Faraggi, M. Tsulaia, Spinor-vector duality in heterotic string orbifolds. JHEP **07**, 004 (2010). https://doi.org/10.1007/JHEP07(2010)004. arXiv:1003.5801
45. A.E. Faraggi, I. Florakis, T. Mohaupt, M. Tsulaia, Conformal aspects of spinor-vector duality. Nucl. Phys. B **848**, 332 (2011). https://doi.org/10.1016/j.nuclphysb.2011.03.002. arXiv:1101.4194
46. A.E. Faraggi, C. Kounnas, S.E.M. Nooij, J. Rizos, Classification of the chiral Z(2) x Z(2) fermionic models in the heterotic superstring. Nucl. Phys. B **695**, 41 (2004). https://doi.org/10.1016/j.nuclphysb.2004.06.030. arXiv:hep-th/0403058
47. B. Assel, K. Christodoulides, A.E. Faraggi, C. Kounnas, J. Rizos, Classification of heterotic Pati–Salam models. Nucl. Phys. B **844**, 365 (2011). https://doi.org/10.1016/j.nuclphysb.2010.11.011. arXiv:1007.2268
48. A. Faraggi, J. Rizos, H. Sonmez, Classification of flipped SU(5) heterotic-string vacua. Nucl. Phys. B **886**, 202 (2014). https://doi.org/10.1016/j.nuclphysb.2014.06.025. arXiv:1403.4107
49. A.E. Faraggi, G. Harries, J. Rizos, Classification of left-right symmetric heterotic string vacua. Nucl. Phys. B **936**, 472 (2018). https://doi.org/10.1016/j.nuclphysb.2018.09.028. arXiv:1806.04434
50. A.E. Faraggi, G. Harries, B. Percival, J. Rizos, Doublet-triplet splitting in fertile left-right symmetric heterotic string vacua. Nucl. Phys. B **953**, 114969 (2020). https://doi.org/10.1016/j.nuclphysb.2020.114969. arXiv:1912.04768
51. A.E. Faraggi, V.G. Matyas, B. Percival, Towards the classification of tachyon-free models from tachyonic ten-dimensional heterotic string vacua. Nucl. Phys. B **961**, 115231 (2020). https://doi.org/10.1016/j.nuclphysb.2020.115231. arXiv:2006.11340
52. A.E. Faraggi, V.G. Matyas, B. Percival, Classification of non-supersymmetric Pati–Salam heterotic string models. Phys. Rev. D **104**, 046002 (2021). https://doi.org/10.1103/PhysRevD.104.046002. arXiv:2011.04113
53. I. Antoniadis, G.K. Leontaris, A supersymmetric $SU(4) \times O(4)$ model. Phys. Lett. B **216**, 333 (1989). https://doi.org/10.1016/0370-2693(89)91125-8
54. A.E. Faraggi, Sterile neutrinos in string derived models. Eur. Phys. J. C **78**, 867 (2018). https://doi.org/10.1140/epjc/s10052-018-6345-4. arXiv:1807.08031
55. A.E. Faraggi, Proton stability in superstring derived models. Nucl. Phys. B **428**, 111 (1994). https://doi.org/10.1016/0550-3213(94)90194-5. arXiv:hep-ph/9403312
56. A.E. Faraggi, Doublet triplet splitting in realistic heterotic string derived models. Phys. Lett. B **520**, 337 (2001). https://doi.org/10.1016/S0370-2693(01)01165-0. arXiv:hep-ph/0107094
57. L. Delle Rose, A.E. Faraggi, C. Marzo, J. Rizos, Wilsonian dark matter in string derived Z' model. Phys. Rev. D **96**, 055025 (2017). https://doi.org/10.1103/PhysRevD.96.055025. arXiv:1704.02579
58. A.E. Faraggi, M. Guzzi, Z's and sterile neutrinos from heterotic string models: exploring Z' mass exclusion limits. Eur. Phys. J. C **82**, 590 (2022). https://doi.org/10.1140/epjc/s10052-022-10539-y. arXiv:2204.11974
59. A.E. Faraggi, M. Guzzi, Extra Z' s and W' s in heterotic-string derived models. Eur. Phys. J. C **75**, 537 (2015). https://doi.org/10.1140/epjc/s10052-015-3763-4. arXiv:1507.07406
60. C. Corianò, A.E. Faraggi, M. Guzzi, Searching for extra Z-prime from strings and other models at the LHC with leptoproduction. Phys. Rev. D **78**, 015012 (2008). https://doi.org/10.1103/PhysRevD.78.015012. arXiv:0802.1792
61. Particle Data Group Collaboration, R.L. Workman et al., Review of particle physics. PTEP **2022**, 083C01 (2022). https://doi.org/10.1093/ptep/ptac097
62. ATLAS Collaboration, G. Aad et al., Measurement of the forward-backward asymmetry of electron and muon pair-production in pp collisions at $\sqrt{s}$ = 7 TeV with the ATLAS detector. JHEP **09**, 049 (2015). https://doi.org/10.1007/JHEP09(2015)049. arXiv:1503.03709
63. LHCb collaboration, R. Aaij et al., Measurement of the forward-backward asymmetry in $Z/\gamma^* \to \mu^+\mu^-$ decays and determination of the effective weak mixing angle. JHEP **11**, 190 (2015). https://doi.org/10.1007/JHEP11(2015)190. arXiv:1509.07645
64. CMS collaboration, A. Tumasyan et al., Measurement of the Drell–Yan forward–backward asymmetry at high dilepton masses in proton-proton collisions at $\sqrt{s}$ = 13 TeV. JHEP **2022**, 063 (2022). https://doi.org/10.1007/JHEP08(2022)063. arXiv:2202.12327
65. J.M. Campbell, R.K. Ellis, An update on vector boson pair production at hadron colliders. Phys. Rev. D **60**, 113006 (1999). https://doi.org/10.1103/PhysRevD.60.113006. arXiv:hep-ph/9905386
66. J.M. Campbell, R.K. Ellis, C. Williams, Vector boson pair production at the LHC. JHEP **07**, 018 (2011). https://doi.org/10.1007/JHEP07(2011)018. arXiv:1105.0020
67. J.M. Campbell, R.K. Ellis, W.T. Giele, A multi-threaded version of MCFM. Eur. Phys. J. C **75**, 246 (2015). https://doi.org/10.1140/epjc/s10052-015-3461-2. arXiv:1503.06182
68. R. Boughezal, J.M. Campbell, R.K. Ellis, C. Focke, W. Giele, X. Liu et al., Color singlet production at NNLO in MCFM. Eur. Phys. J. C **77**, 7 (2017). https://doi.org/10.1140/epjc/s10052-016-4558-y. arXiv:1605.08011
69. J. Campbell, T. Neumann, Precision phenomenology with MCFM. JHEP **12**, 034 (2019). https://doi.org/10.1007/JHEP12(2019)034. arXiv:1909.09117
70. S. Camarda et al., DYTurbo: fast predictions for Drell–Yan processes. Eur. Phys. J. C **80**, 251 (2020). https://doi.org/10.1140/epjc/s10052-020-7757-5. arXiv:1910.07049
71. R. Gavin, Y. Li, F. Petriello, S. Quackenbush, FEWZ 2.0: a code for hadronic Z production at next-to-next-to-leading order. Comput. Phys. Commun. **182**, 2388 (2011). https://doi.org/10.1016/j.cpc.2011.06.008. arXiv:1011.3540
72. Y. Li, F. Petriello, Combining QCD and electroweak corrections to dilepton production in FEWZ. Phys. Rev. D **86**, 094034 (2012). https://doi.org/10.1103/PhysRevD.86.094034. arXiv:1208.5967
73. T.-J. Hou et al., New CTEQ global analysis of quantum chromodynamics with high-precision data from the LHC. arXiv:1912.10053
74. S. Alekhin, J. Blümlein, S. Moch, R. Placakyte, Parton distribution functions, α_s, and heavy-quark masses for LHC Run II. Phys. Rev. D **96**, 014011 (2017). https://doi.org/10.1103/PhysRevD.96.014011. arXiv:1701.05838
75. S. Bailey, T. Cridge, L.A. Harland-Lang, A.D. Martin, R.S. Thorne, Parton distributions from LHC, HERA, tevatron and fixed target data: MSHT20 PDFs. Eur. Phys. J. C **81**, 341 (2021). https://doi.org/10.1140/epjc/s10052-021-09057-0. arXiv:2012.04684
76. NNPDF Collaboration, R.D. Ball et al., The path to proton structure at 1% accuracy, Eur. Phys. J. C **82**, 428 (2022). https://doi.org/10.1140/epjc/s10052-022-10328-7. arXiv:2109.02653
77. J.C. Collins, D.E. Soper, Angular distribution of dileptons in high-energy hadron collisions. Phys. Rev. D **16**, 2219 (1977). https://doi.org/10.1103/PhysRevD.16.2219
78. L.T. Brady, A. Accardi, W. Melnitchouk, J.F. Owens, Impact of PDF uncertainties at large x on heavy boson production. JHEP **06**, 019 (2012). https://doi.org/10.1007/JHEP06(2012)019. arXiv:1110.5398
79. S. Amoroso et al., Snowmass 2021 whitepaper: proton structure at the precision frontier. arXiv:2203.13923